ICWE 16
August 27-31, 2023
FLORENCE - ITALY
16th International
Conference on
Wind Engineering

Advancements in the physical simulation of atmospheric surface layer flows using synthetic turbulence modulation in a large boundary layer wind tunnel

Ryan A. Catarelli [1], Yutiwadee Pinyochotiwong [2], Forrest J. Masters [3], Brian M. Phillips [4], Tai-An Chen [5], Jennifer A. Bridge [6], Kurtis R. Gurley [7]

[1]*University of Florida, Gainesville, United States, rcatarelli@ufl.edu*
[2]*University of Florida, Gainesville, United States, y.pinyochotiwong@ufl.edu*
[3]*University of Florida, Gainesville, United States, masters@eng.ufl.edu*
[4]*University of Florida, Gainesville, United States, brian.phillips@essie.ufl.edu*
[5]*University of Florida, Gainesville, United States, chen571@ufl.edu*
[6]*University of Florida, Gainesville, United States, jennifer.bridge@essie.ufl.edu*
[7]*University of Florida, Gainesville, United States, kgurl@ce.ufl.edu*

SUMMARY

This work presents continued advancements in the development of a high-performance multi-fan array used in conjunction with traditional passive control devices in a large boundary layer wind tunnel with the goal of improving reduced geometric scale physical simulations of complex turbulent flows observed in the atmospheric surface layer.

Keywords: multi-fan, synthetic turbulence modulation, closed-loop control

1. INTRODUCTION

This work presents continued advancements in the development of a high-performance multi-fan array used in conjunction with traditional passive control devices (e.g., a roughness element grid) in a large boundary layer wind tunnel (BLWT) with the goal of improving reduced geometric scale physical simulations of complex turbulent flows observed in the atmospheric surface layer (ASL).

Traditional BLWT flow simulations are known to be deficient in low frequency energy content for large model scales (Mooneghi et al., 2016), which may affect the separation zones on model structures and introduce errors in the estimation of peak wind loading. This work demonstrates that high Reynolds number active turbulence control in large BLWTs can compensate for this deficiency for well understood neutrally stratified boundary layer (BL) flows.

2. METHODOLOGY

Generating the necessary low frequency energy content at model-scale requires physical simulation equipment capable of modulating turbulence characteristics to achieve kinematic similitude with full-scale wind phenomena. In addition, flow control software capable of converging on simultaneous simulation targets, such as the profiles of mean, turbulence, and integral length scales, as well as longitudinal turbulence spectra, is critical. To achieve this goal, turbulence was synthetically generated using spectral models and injected into the vaneaxial fan-driven flow using a multi-fan array with very low rotor inertia and fast response characteristics. Errors between input target spectra and measured output spectra were iteratively reduced using spectral warping techniques. A governing convergence algorithm (GCA) was added to balance the control inputs to the main BLWT fans, multi-fan array, and automated roughness grid.

2.1. Experimental configuration

Data collection was carried out in the BLWT located at the University of Florida's Experimental Facility (UFEF), which is part of the National Science Foundation's (NSF) Natural Hazards Engineering Research Infrastructure (NHERI) program. The UF BLWT is a long-fetch low-speed open circuit tunnel with dimensions of 6 m W x 3 m H x 38 m L (see Fig. 1). The GCA control system implemented at the UF BLWT automatically configures the multi-stage flow conditioning system to achieve user-specified velocity profiles difficult to produce by traditional means.

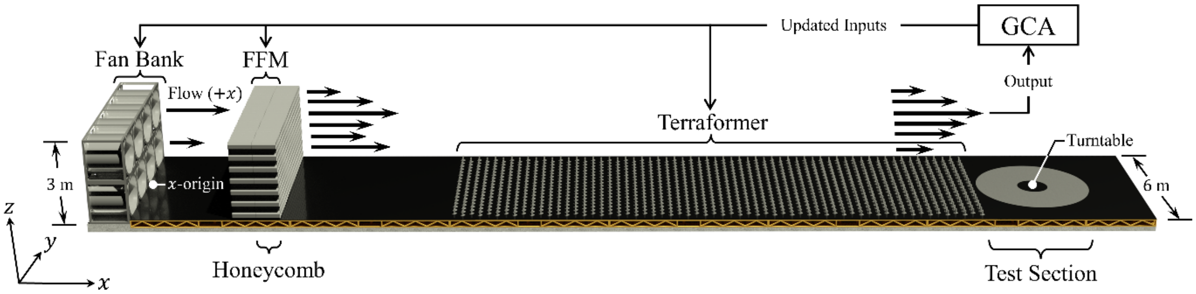

Figure 1. Multi-stage flow conditioning system at UF BLWT.

Eight Aerovent 54D5 VJ vaneaxial fans (VAF) driven by 56 kW AC induction motors generate air flow in the tunnel. Ambient intake air is pre-conditioned by a nested honeycomb system to reduce fan-generated turbulence and ensure horizontal homogeneity of the velocity profile before entering the development section of the wind tunnel. The 1116 mechanized roughness elements configured in a 62x18 array, called the Terraformer (TF) (Catarelli et al., 2020; Fernández-Cabán and Masters, 2017), induce surface drag to achieve desired upwind terrain conditions. The multi-fan array, referred to as the Flow Field Modulator (FFM), consists of 319 individually controlled shrouded propeller assemblies driven by 800-Watt brushless DC motors with electronic speed controllers. The FFM produces rapid velocity changes and can generate profile shapes that vertically extend and/or deviate from neutral BL profiles naturally grown over grid roughness.

A multi-degree-of-freedom automated instrument traverse in the UF BLWT can position multi-hole velocity probes laterally, vertically, and longitudinally in the test section. Three Turbulent Flow Instrumentation (TFI) Series 100 Cobra Probes collected flow measurements with a 30-second sampling period at each height. Once the measured profile converged on a given target, the converged profile was recollected using a 2-minute sampling period at each height for improved quantification of turbulence characteristics.

2.2. Turbulence control process

The proposed turbulence control process is primarily based on the power spectral warping method used in Cao et al. (2002) with modifications to account for differences in facility configurations (e.g., long fetch, high-performance control equipment, and size of the UF BLWT). Use of the iterative GCA was demonstrated in previous studies to successfully converge longitudinal mean velocity (U) profiles. In the present study, the GCA is combined with a modified spectral-based approach to also converge on properties derived from the longitudinal fluctuating component. The iterative procedure increases input energy into the flow via the FFM at targeted deficient frequencies until desired turbulence characteristics are reached.

3. EXPERIMENTAL STUDY

3.1. Simulation targets

The present study targets the along-wind vertical profiles of U, standard deviation (σ_u), integral length scale (L_u^x) with turbulence spectra (S_{uu}): the U profile is described by the log law

$$U(z) = \frac{u_*}{\kappa} \ln\left(\frac{z-d}{z_0}\right) \tag{1}$$

where u_* is shear velocity, κ is the von Kármán constant, d is zero-plane displacement, z_0 is aerodynamic roughness length, and z is height; σ_u is described by

$$\sigma_u(z) = Au_* = \frac{\kappa A}{\ln\left(\frac{z-d}{z_0}\right)} U(z) \tag{2}$$

where A is a constant (equal to 2.5); and $L_u^x(z)$ and $S_{uu}(n, z)$ are both taken from ESDU 85020 (1985).

3.2. Results

Converged profiles of a 1:100 scale ASCE Exposure B (z_0 = 0.3 m full-scale) target approach flow are shown in Fig. 2 along with GCA input commands. The shaded blocks shown in the first three plots of the figure represent the input commands of VAF, FFM, and TF, from left to right respectively. The blue and the orange shades refer to positive and negative fan speeds, respectively. The input heights of TF elements are illustrated by the height of the grey blocks of six zones in the bottom of the third plot. The subsequent plots in the figure present resulting $U(z)$, $\sigma_u(z)$, $I_u(z)$, and $L_u^x(z)$ profiles, respectively. The black line in each plot is the corresponding target profile.

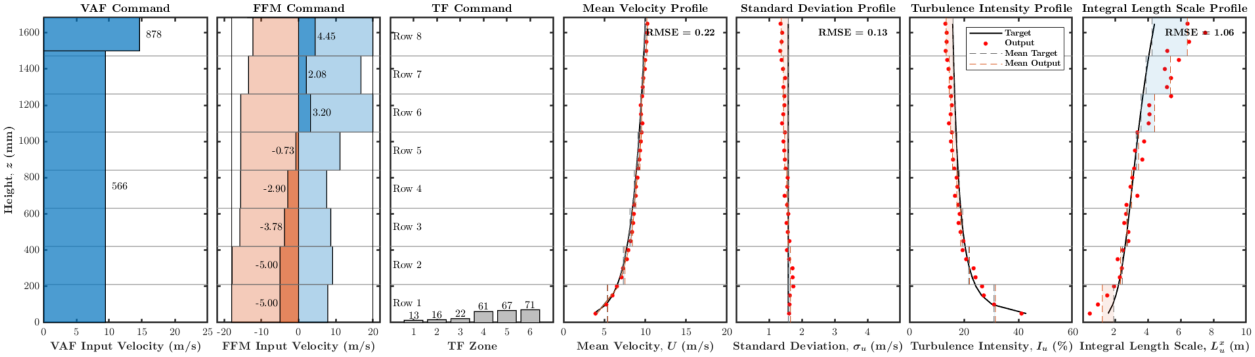

Figure 2. The plots of VAF, FFM, and TF input commands, and the resulting flow characteristics with target profiles at the converged stage of the Exposure B target.

Power spectral densities (PSD) for the longitudinal fluctuating components of the FFM input commands, measurement data, and targets are shown in Fig. 3. The eight black circles shown in the U profile (first column of Fig.3) indicate the middle height of each FFM cell row, where the PSDs were calculated. The black lines, blue lines, and red lines correspond to the target quantities, FFM inputs, and measurement data, respectively. For the first iteration, the resulting spectra were considerably deficient in the low frequency range indicating a need to increase the input energy in the next iteration. In the final iteration, the measured spectra matched the target spectra well.

4. CONCLUSIONS

The present study demonstrates the capability of the UF BLWT to produce neutrally stratified BL flows with sufficient low frequency energy content, while preserving characteristic spectral shapes. The ultimate goal for this system is to reproduce the relevant characteristics of time-varying non-synoptic flow fields either as-measured in-situ or modeled by potential users of the UF facility. Along with the continued development of this system, new high-throughput flow measurement tools currently being developed at the facility will reduce data collection and profile convergence time by a factor of four to accelerate the rate of experimental discovery.

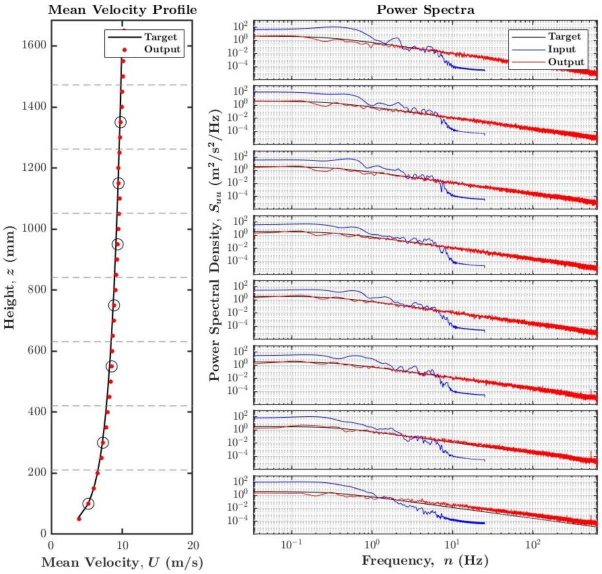

Figure 3. The plots of U profile and S_{uu} at the converged stage of the Exposure B target.

ACKNOWLEDGEMENTS

Support for this research was provided by the NSF MRI program (CMMI-1428954) with additional support for experimentation through the NSF NHERI program (NHERI, CMMI-2037725). The authors also wish to recognize the Powell Structures and Materials Laboratory staff for their invaluable contributions to instrument design, construction, and wind tunnel testing. Any opinions, findings, and conclusions or recommendations expressed in this work are those of the authors and do not necessarily reflect the views of the sponsors, partners, and contributors.

REFERENCES

Cao, S., Nishi, A., Kikugawa, H., and Matsuda, Y., 2002. Reproduction of wind velocity history in a multiple fan wind tunnel. Journal of Wind Engineering and Industrial Aerodynamics, 90(12–15), 1719–1729.

Catarelli, R. A., Fernández-Cabán, P. L., Masters, F. J., Bridge, J. A., Gurley, K. R., and Matyas, C. J., 2020. Automated terrain generation for precise atmospheric boundary layer simulation in the wind tunnel. Journal of Wind Engineering and Industrial Aerodynamics, 207, Article 104276.

ESDU 85020, 1985. Characteristics of atmospheric turbulence near the ground. Part II: Single point data for strong winds (neutral atmosphere).

Fernández-Cabán, P. L., and Masters, F. J., 2017. Near surface wind longitudinal velocity positively skews with increasing aerodynamic roughness length. Journal of Wind Engineering and Industrial Aerodynamics, 169, 94–105.

Mooneghi, M. A., Irwin, P., and Chowdhury, A. G., 2016. Partial turbulence simulation method for predicting peak wind loads on small structures and building appurtenances. Journal of Wind Engineering and Industrial Aerodynamics, 157, 47-62.